THE AMERICAN SOCIETY OF MECHANICAL ENGINEERS
345 E. 47th St., New York, N.Y. 10017

NUMERICAL AND EXPERIMENTAL EVALUATION OF TURBULENT MODELS FOR NATURAL CONVECTION SIMULATION IN A THERMALLY DRIVEN SQUARE CAVITY

C. Béghein
CETHIL URA CNRS 1372
INSA
Villeurbanne, France

F. Penot and S. Mergui
LET URA CNRS 1430
Université de Poitiers
Poitiers, France

F. Allard
LMCPB
Université de La Rochelle
La Rochelle, France.

ABSTRACT

Natural convection in a thermally driven square cavity filled with air is studied numerically. Since the thermal Rayleigh number of the configuration ranges between 10^8 and 10^{12}, the flow is turbulent and k-ε models are used to predict the behavior of the flow. For this natural convection problem, the viscous sublayer must be discretized and the behavior of the turbulent quantities is damped within this sublayer through low-Reynolds number modelling. Two models are evaluated in detail (the model proposed by Henkes and Hoogendoorn for the EUROTHERM/ERCOFTAC workshop organised in 1992 and the low-Reynolds number model developed by Abrous) and one model is compared for one point (the low-Reynolds number model proposed by Chien). An evaluation of these models is first performed. The average heat transfer rate, the maximum vertical velocity, the vertical thermal stratification at cavity center computed with the Henkes and Hoogendoorn model and the Abrous model highlight different behavior of these models, especially in the range of the transition Rayleigh number. A computation performed with all models tested for a Rayleigh number of 10^{10} stresses these differences. Numerical results obtained with the Henkes and Hoogendoorn model and the Abrous model for a Rayleigh number of 1.7×10^9 are next compared with experimental results obtained in an air filled cavity (1m×1m vertical section). Three different simulations have been carried out considering adiabatic or perfectly conductive horizontal walls. Even if the heat losses through the cavity walls are extremely small, the comparison of velocity and temperature measurements with numerical simulation shows the influence of the vertical gradient of temperature existing in the experimental cavity. A good agreement between experimental and numerical results is shown for the Abrous model but the Henkes model overestimates the diffusion process as predicted in the former part of this study.

NOMENCLATURE

$C_{1\varepsilon}, C_{2\varepsilon}, C_{3\varepsilon}, C_\mu$	Constants in the k-ε model.
D	Cavity depth (experimental cell).
f_1, f_2, f_μ	Damping functions in the k-ε model.
g	Gravitational acceleration.
Gr_T	Thermal Grashof number, $g\beta_T\Delta TH^3/\nu^2$.
H	Cavity height.
k	Turbulent kinetic energy.
k^*	Non-dimensional turbulent kinetic energy $(k/(g\beta_T\Delta TH))$.
Nu	Nusselt number.
p	Pressure.
p^*	Non-dimensional pressure $(p/(\rho g\beta_T\Delta TH))$.
Pr	Prandtl number, ν/α.
R_t	Turbulent Reynolds number.
Ra_T	Thermal Rayleigh number, $g\beta_T\Delta TH^3/\nu\alpha$.
T	Temperature.
T^*	Non-dimensionaltemperature$((T-T_C)/(T_H-T_C))$.
T_C, T_H	Temperatures of the right and left vertical walls.
u_i	Velocity components.
u_i^*	Non-dimensional velocity components $(u_i/(g\beta_T\Delta TH)^{0.5})$.
W	Cavity width.
x_i	Coordinates.
x_i^*	Non-dimensional coordinates (x_i/H).

Greek letters

α	Thermal diffusivity of the fluid.
β_T	Coefficient of volumetric expansion due to temperature change.
δ_{j2}	Kronecker symbol.

Presented at the ASME Winter Annual Meeting
New Orleans, Louisiana — November 28—December 3, 1993

ΔT	Temperature difference between hot and cold walls (T_H-T_C).
ε	Dissipation rate of turbulent kinetic energy.
ε^*	Non-dimensional dissipation rate of turbulent kinetic energy ($\varepsilon H/(g\beta_T \Delta TH)^{1.5}$).
ν	Kinematic viscosity of the fluid.
ν_t	Turbulent viscosity.
ν_t^*	Non-dimensional turbulent viscosity (ν_t/ν).
ρ	Fluid density.
σ_k	Turbulent Prandtl number for turbulent kinetic energy.
σ_T	Turbulent Prandtl number for temperature.
σ_ε	Turbulent Prandtl number for the dissipation rate of turbulent kinetic energy.

Superscripts

*	Refers to non-dimensional value.
-	Refers to time-average value.

Subscripts

C	Refers to cold wall.
H	Refers to hot wall.

INTRODUCTION

During the past thirty years, natural convection has been the subject of a large amount of numerical and experimental studies. Heat transfer by natural convection occurs in a wide range of engineering applications such as meteorology, astrophysics, thermonuclear reactors, electronics, and more particularly building physics (Allard et al., 1991), (Allard et al., 1992), (Béghein, 1992). In dwelling cells, the flow becomes unstable and turbulent numerical models are necessary to predict the behavior of such flows. k-ε models based on time-averaging of velocities and temperatures are usually adopted for these types of flows. For forced convection configurations, the use of wall laws avoids the discretization of the viscous sublayer and a rather small amount of grid nodes can be sufficient to obtain satisfactory results. Unfortunately, such wall laws are not adapted to natural convection problems. The viscous sublayer must therefore be discretized, the behavior of turbulent variables is damped within the whole discretization domain through low-Reynolds number modelling.

Until now, many low-Reynolds number k-ε models have been proposed but they seem to give different results for identical configurations. Fraikin et al. (1980), Nobile et al. (1989) and Lankhorst (1991) have compared numerical results obtained with k-ε models without damping functions but which include molecular viscous and thermal diffusion processes to experimental results. Fraikin et al. (1980) focused on numerical modelling of convection for the "Conductive Window Problem" configuration. They scaled the heat transfer rate integrated over the hot wall with $Gr_L^{0.273}$, which corresponds to the one found through experimental means. A sensitivity analysis dealing with the constants of the turbulent conservation equations shows their significant influence on the behavior of the turbulent quantities. Nobile et al. (1989) performed the same study for the "Adiabatic Window Problem" configuration. The characteristic scale used to quantify the average heat transfer rate, for a rather narrow range of thermal Rayleigh numbers (10^7-10^{10}), is $Ra_T^{1/3}$. This correlation is in good agreement with the one experimentally obtained by Cheesewright and Ziai (1986) for a cavity filled with a fluid which Prandtl number is close to unity. Lankhorst (1991) presented a very interesting comparison of numerical and experimental results (cavity with a 1 by 1 meter square cross section, experiments were performed at several temperature differences) for the "Adiabatic Window Problem" and "Conductive Window Problem" two- and three-dimensional configurations. For Rayleigh numbers above 2×10^9, the flow was found to be turbulent and the best agreement was for three-dimensional computations.

Low-Reynolds number model evaluations have been performed by many authors. Among these are Patel et al. (1981,1985), Betts and Dafa'Alla (1986), Henkes (1990), Chen et al. (1990). A systematic evaluation of the performance of eight low-Reynolds number k-ε models, based on the consistance of their damping functions and source terms with their approximate expressions obtained from Taylor series expansions close to a solid wall, has been realised by Patel et al. (1981,1985). The models which perform the best are the Launder and Sharma (1974), the Chien (1982) and the Lam and Bremhorst (1981) models. An improvement of f_μ, f_1 and f_2 damping functions may still increase the accuracy of these results. The configuration chosen by Betts and Daffa'Alla (1986) for an evaluation of nine low-Reynolds number k-ε models is a high aspect ratio air-filled cavity (the flow is one-dimensional at half the cavity height). The comparison with experimental results in terms of average velocity and temperature distributions, maximum vertical velocity and average Nusselt number shows a good agreement for the Jones and Launder (1972) and the Launder and Sharma (1974) models. Henkes (1990) performed the same kind of evaluation for an air- or water-filled square cavity under the "Adiabatic Window Problem" configuration, and for a wide range of thermal Rayleigh numbers (up to 10^{15}). In this study, Henkes shows that an increase in the Prandtl number induces an increase in the laminar-turbulent transition Rayleigh number and that this Rayleigh number differs according to the low-Reynolds number k-ε model considered. Moreover, the solutions obtained do not seem to be unique. The comparison of the computed average Nusselt number with the experimental ones determined by Tsuji and Nagano (1989) (plane vertical plate) and Betts and Daffa'Alla (1986) (high aspect ratio enclosure) gives the best concordance for the Chien (1982) and the Jones and Launder (1972) models. The numerical evaluation of Chen et al. (1990) deals with the evaluation of the Lam and Bremhorst (1981) low-Reynolds number k-ε model and a high-Reynolds number k-ε model for the numerical simulation of a turbulent flow in a small scale square cavity filled with water and a tall rectangular cavity filled with air. The low-Reynolds number model of Lam and Bremhorst gives the best concordance for the vertical velocity at half the cavity height and the wall heat transfer rates.

The aim of the present paper is to describe the results of a numerical and experimental evaluation of three low-Reynolds number k-ε models and to select one for the numerical modelling of weakly turbulent flows in confined spaces such as those

encountered in buildings. The different behaviors of the three models are first stressed, for a thermal Rayleigh number range of 10^8-10^{12}. The comparison with experimental results obtained for an air-filled square cavity which thermal Rayleigh number is 1.7×10^9 enables us then to select one of these models.

PHYSICAL AND NUMERICAL MODELS

Physical model

The physical model is an air-filled square cavity with adiabatic or perfectly conducting horizontal walls, and vertical isothermal walls submitted to different temperature levels, as illustrated in Figure 1. The thermal Rayleigh number of the configuration, based on the cavity height and the temperature difference between the vertical walls, ranges between 10^8 and 10^{12}. The Prandtl number of the fluid considered is 0.71.

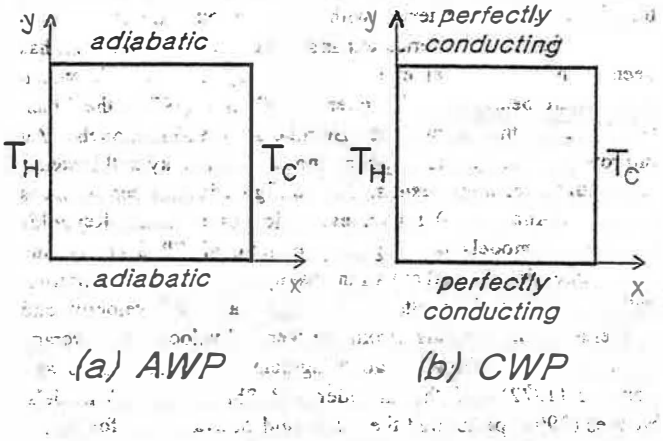

FIGURE 1 : PHYSICAL MODEL STUDIED, (a) ADIABATIC HORIZONTAL WALLS, (b) PERFECTLY CONDUCTING HORIZONTAL WALLS (T_H>T_C).

Governing equations

The turbulent behavior of the flow is modelled via the eddy viscosity concept proposed by Boussinesq which relates the turbulent stresses $-\overline{u'_iu'_j}$ to the mean velocity gradients. The turbulent heat fluxes $-\overline{u'_jT'}$ are expressed from Reynolds analogy between momentum and heat. The turbulent viscosity is calculated in each point of the cavity from the two-equation k-ε model. The resulting equations written in their dimensionless form are as follows (incompressible flow, Boussinesq approximation):

Continuity

$$\frac{\partial \overline{u_i^*}}{\partial x_i^*}=0 \qquad (1)$$

Momentum

$$\overline{u_j^*}\frac{\partial \overline{u_i^*}}{\partial x_j^*}=-\frac{\partial \overline{p^*}}{\partial x_i^*}+\frac{1}{Gr_T^{1/2}}\frac{\partial}{\partial x_j^*}\left[(1+\nu_t^*)\frac{\partial \overline{u_i^*}}{\partial x_j^*}\right]+S_{\overline{u_i^*}} \qquad (2)$$

$$S_{\overline{u_i^*}}=\frac{1}{Gr_T^{1/2}}\frac{\partial}{\partial x_j^*}\left[(1+\nu_t^*)\frac{\partial \overline{u_j^*}}{\partial x_i^*}\right]+\delta_{i2}(\overline{T^*}-0.5)-\frac{2}{3}\frac{\partial k^*}{\partial x_i^*} \qquad (3)$$

Energy

$$\overline{u_j^*}\frac{\partial \overline{T^*}}{\partial x_j^*}=\frac{1}{Gr_T^{1/2}}\frac{\partial}{\partial x_j^*}\left[\left(\frac{1}{Pr}+\frac{\nu_t^*}{\sigma_T}\right)\frac{\partial \overline{T^*}}{\partial x_j^*}\right] \qquad (4)$$

Turbulent kinetic energy

$$\overline{u_j^*}\frac{\partial k^*}{\partial x_j^*}=\frac{1}{Gr_T^{1/2}}\frac{\partial}{\partial x_j^*}\left[\left(1+\frac{\nu_t^*}{\sigma_k}\right)\frac{\partial k^*}{\partial x_j^*}\right]+S_{k^*} \qquad (5)$$

$$S_{k^*}=\frac{1}{Gr_T^{1/2}}(P_k+G_k)-\epsilon^*+D^* \qquad (6)$$

Dissipation rate of turbulent kinetic energy

$$\overline{u_j^*}\frac{\partial \epsilon^*}{\partial x_j^*}=\frac{1}{Gr_T^{1/2}}\frac{\partial}{\partial x_j^*}\left[\left(1+\frac{\nu_t^*}{\sigma_\epsilon}\right)\frac{\partial \epsilon^*}{\partial x_j^*}\right]+S_{\epsilon^*} \qquad (7)$$

$$S_{\epsilon^*}=\frac{1}{Gr_T^{1/2}}[C_{1\epsilon}f_1(P_k+C_{3\epsilon}G_k)]\frac{\epsilon^*}{k^*}-C_{2\epsilon}f_2\frac{\epsilon^{*2}}{k^*}+E^* \qquad (8)$$

Turbulent viscosity

$$\nu_t^*=Gr_T^{1/2}C_\mu f_\mu\frac{k^{*2}}{\epsilon^*} \qquad (9)$$

with

$$P_k=\frac{\nu_t^*}{2}\left(\frac{\partial \overline{u_i^*}}{\partial x_j^*}+\frac{\partial \overline{u_j^*}}{\partial x_i^*}\right)^2,\quad G_k=-\frac{\nu_t^*}{\sigma_T}\frac{\partial \overline{T^*}}{\partial x_j^*}\delta_{j2} \qquad (10)$$

The variables of the stated problem are made non-dimensional with the cavity height, the temperature difference between vertical hot and cold walls, the buoyant velocity, the kinematic viscosity of the fluid considered. As a heavy under-relaxation is employed to ensure convergence, the steady state formulation is used.

The constants $C_{1\varepsilon}$, $C_{2\varepsilon}$, $C_{3\varepsilon}$, C_μ, the damping functions f_1, f_2, f_μ and the source terms D^* and E^* differ according to the k-ε model tested. The turbulent Prandtl number for the temperature (σ_T), the turbulent kinetic energy (σ_k), the dissipation rate of turbulent kinetic energy (σ_ε) are assigned the following values :

$$\sigma_T=0.9, \quad \sigma_k=1.0, \quad \sigma_\varepsilon=1.3 \tag{11}$$

The k-ε models tested

In this study, three k-ε models are investigated:

- the model proposed by Henkes and Hoogendoorn within the frame of the EUROTHERM-ERCOFTAC workshop that they organised in Delft in April 1992 (Henkes et al., 1992), (Béghein et al., 1992),
- the low-Reynolds number model developed by Abrous et al. (1984),
- the low-Reynolds number model developed by Chien (1982).

The k-ε model proposed by Henkes and Hoogendoorn is intermediate between high and low-Reynolds number models. No wall laws are used to avoid the discretization of the viscous sublayer, the laminar behavior of velocities, temperature and turbulent quantities in this region is accounted for by the introduction of molecular diffusion terms in each conservation equation. The constants, source terms and turbulent boundary conditions of this model are the following:

$$C_{1\varepsilon}f_1=1.44, \quad C_{2\varepsilon}f_2=1.92, \quad C_{3\varepsilon}=\tanh\left|\overline{v^*}/\overline{u^*}\right|, \quad C_\mu f_\mu=0.09$$
$$D^*=E^*=0, \quad k_W^*=0, \quad \varepsilon_W^*=\infty \tag{12}$$

In the model developed by Abrous et al.(1984), the behavior of the turbulent viscosity is damped through f_μ function which depends on the turbulent local Reynolds number based on turbulent variables. The influence of f_μ acts therefore on the whole discretization domain. The constants and damping functions are as recommended by Launder and Spalding(1974):

$$C_{1\varepsilon}f_1=1.44, \quad C_{2\varepsilon}f_2=1.92$$
$$C_{3\varepsilon}=0.7+(0.7-1.44)\left|\overline{u^*}\right|/\sqrt{\overline{u^{*2}}+\overline{v^{*2}}} \tag{13}$$
$$C_\mu f_\mu=0.09\exp\left[-3.4/(1+R_t/50)^2\right] \quad with \quad R_t=Gr_T^{1/2}k^{*2}/\varepsilon^*$$

Source terms D^* and E^* of k^* and ε^* conservation equations are zero. The boundary conditions for k^* and ε^* are as proposed by To and Humphrey(1986):

$$k_W=0, \quad \varepsilon_W^*=2Gr_T^{-1/2}\left(\frac{\partial k^{*1/2}_W}{\partial y^*}\right)^2 \tag{14}$$

In the low-Reynolds number model developed by Chien(1982), the dissipation rate of turbulent kinetic energy is zero at the wall. Therefore, extra terms D^* and E^* are included in the conservation equations for k^* and ε^*. Moreover, the behavior of the turbulent viscosity and the destruction of the dissipation rate of turbulent kinetic energy are damped through f_μ and f_2 functions, which respectively act on the viscous sublayer alone and the whole discretization domain. The extra terms D^* and E^*, the constants and damping functions of this model are calculated as follows:

$$D^*=-2Gr_T^{-1/2}\frac{k^*}{x^{*2}}, \quad E^*=-2Gr_T^{-1/2}\frac{\varepsilon^*}{x^{*2}}\exp(-0.5x^{**})$$
$$with \quad x^{**}=\sqrt{\left(\frac{\partial u_t^*}{\partial x^*}\right)_W}\,Gr_T^{1/4} \tag{15}$$
$$C_{1\varepsilon}f_1=1.35, \quad C_{3\varepsilon}=\tanh\left|\overline{v^*}/\overline{u^*}\right|$$
$$C_{2\varepsilon}f_2=1.8[1-0.22\exp(-(R_t/6)^2)]$$
$$C_\mu f_\mu=0.09[1-\exp(-0.0115x^{**})]$$

where x^* is the distance to the closest wall and u_t^* is the velocity component tangential to that wall.

Numerical procedure

The numerical resolution procedure of the equations which couple the pressure, velocities, temperature and turbulent quantities is the SIMPLER (Semi Implicit Method for Pressure Linked Equations Revised) algorithm developed by Patankar(1980). The model equations are spatially discretized over a staggered grid using the finite difference method and then integrated over control volumes. The Power-Law scheme is employed for the treatment of the convective-diffusive fluxes. The line-by-line Tri-Diagonal Matrix Algorithm (Anderson et al., 1983) is used to solve the linearized equations. Convergence of the SIMPLER algorithm is reached when the residuals of all the equations are below a specified tolerance (between 10^{-7} and 10^{-8}). At least 5000 iterations are necessary to obtain convergence, which corresponds to a CPU time of about 22 minutes on an IBM3090 computer (vectorization mode, 48×48 grid). As recommend d by Henkes and Hoogendoorn within the frame of EUROTHERM-ERCOFTAC workshop, a hyperbolic grid point distribution for the horizontal direction and a sinusoidal grid point distribution for the vertical direction have been used. With such distributions, a 48×48 grid ensures at least 3 grid points between the wall and the location of maximum velocity, for a thermal Rayleigh number equal or less than 10^{12}. For the "Adiabatic Window Problem" configuration and a hermal Rayleigh number of 5×10^{10}, such a grid point distribution led to a good agreement with the reference solution obtained by Henkes and Hoogendoorn within the frame of the EUROTHERM-ERCOFTAC workshop (Béghein et al., 1992).

EXPERIMENTAL FACILITY

The experimental cell is 1.04 meter wide, the vertical aspect ratio H/W is 0.9, the horizontal aspect ratio D/W is 0.3. The temperature difference between the vertical active walls is 20°C. Temperature levels imposed on the hot and cold walls were chosen symmetrically with respect to the room temperature

(20°C), so that T_H=30°C and T_C=10°C. The thermal Rayleigh number based on cavity height, temperature difference between vertical walls and physical properties of air at the mean reference temperature $(T_H+T_C)/2$ is thus 1.7×10^9. In order to avoid radiative and conductive heat transfer considerations, spatially and temporally uniform temperature levels were imposed on the active walls. The other four walls were considered to be passive: their temperature was not controlled, although they were designed to provide a high degree of thermal insulation. A schematic view is presented in Figure 2.

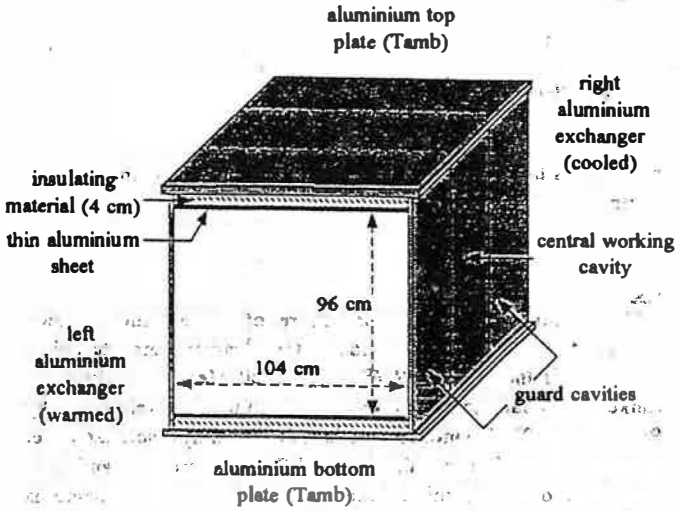

FIGURE 2 : SCHEMATIC VIEW OF THE CAVITY.

The two active walls of the cavity were composed of two plane aluminium heat-exchangers in which water circulated at high speed. For each of these walls, circulation was produced by a pump with a flow which characteristics were calculated in order to obtain constant uniform temperatures within ±0.2°C along the entire height of the wall. The temperature of these two water circuits was regulated using two thermostatically controlled baths, allowing a temperature range between -10°C and 60°C. Wall temperatures were monitored by two thermocouples at the inlet and the outlet of each exchanger. The walls were carefully polished in order to minimize radiation exchanges (ε=0.2).

The cavity was divided into three sections in order to better approximate adiabatic conditions on the passive vertical walls: a 300 mm deep central cavity flanked by two 200 mm deep guard cavities intended to limit end effects by reproducing a flow identical to that obtained in the central cavity. The symmetry of this configuration provided the desired adiabatic conditions on the vertical partition walls. A 20 mm thick space of air outside the guard cavities increased the thermal insulation of these passive walls. All these vertical partition walls were composed of thin (2 mm) sheets of transparent Macrolon, allowing for visualizations and L.D.A. velocity measurements. In addition, except when imaging was performed, insulation panels were placed on the outside in which openings had been made to allow laser beams to pass through during velocity measurements.

The upper and lower horizontal walls were composed of aluminium exchangers but without interior water circulation. Polystyrene plates (50 mm thick) were glued on their inner surfaces. These insulating layers were covered with a thin (5 μm) sheet of aluminium to limit radiation effects (ε=0.07). An insulating layer (150 mm thick) was also glued on each outer exchanger surface to minimize heat transfer with the outside.

A 15 mm wide groove along the entire length of the cavity ceiling contained a sliding metal band with an attached vertical 1.5 m rod. The probe used for temperature measurements was attached to one end of the rod, and the other end was connected to a two-dimensional (vertical and horizontal) computer-controlled positioning system. The groove was located along the edge of the central working cavity, as close as possible to one of the separating walls. The device allowed complete scanning of the cavity without any significant flow disturbance in the median plane where the measurements were performed.

RESULTS AND DISCUSSION

Numerical evaluation of the three k-ε models

We first performed simulations for the three k-ε models tested and for the Adiabatic Window Problem (AWP) configuration . The k-ε model proposed by Henkes and Hoogendoorn was easier to converge than the other models, due to rather high values of turbulent viscosity. The Rayleigh number range investigated with this model was between 10^8 and 10^{12}. With a larger under-relaxation, we could obtain converged results with the Abrous model over a more restricted range of Rayleigh numbers (between 10^9 and 10^{11}). With the Chien model, only one simulation could be performed ($Ra_T=10^{10}$).

For all simulations performed, we calculated the average Nusselt number at the hot wall, the maximum vertical velocity at half the cavity height, the thermal stratification at cavity center. Figure 3 depicts the evolution of the average Nusselt number for the thermal Rayleigh number range investigated (Henkes and Hoogendoorn or "standard" model, Abrous model). At moderate values of the thermal Rayleigh number, the Nusselt number scaled with $Ra_T^{1/3}$ decreases until a minimum value which corresponds to a Rayleigh number of 10^9 for the Henkes and Hoogendoorn model and 10^{10} for the Abrous model. These Rayleigh numbers are representative of the transition to unsteady natural convection predicted by both models. For higher Rayleigh numbers, $Nu/Ra_T^{1/3}$ linearly increases under the fully turbulent regime for the Henkes and Hoogendoorn model and remains constant for the Abrous model. In Figure 4, we plotted the thermal stratification $\partial T^*/\partial y^*$ at cavity center as a function of the thermal Rayleigh number. In the laminar range, the thermal stratification predicted by both models increases while it decreases in the turbulent regime. In the turbulent regime, the flow at cavity center is much more stratified for the Abrous model than for the Henkes and Hoogendoorn model. In Figure 5, which represents the maximum vertical velocity at half the cavity height as a function of the thermal Rayleigh number, one can remark two different behaviors in the

laminar regime. While the maximum vertical velocity computed with the Abrous model increases in the laminar regime, it decreases for the Henkes and Hoogendoorn model. In the turbulent range, the evolutions predicted by both models are similar; for high Rayleigh numbers, both models seem to predict identical values of the maximum vertical velocity. Moreover, due to the stronger diffusion process predicted by the Henkes and Hoogendoorn model, the maximum vertical velocity computed by this model is smaller than the one computed by the Abrous model.

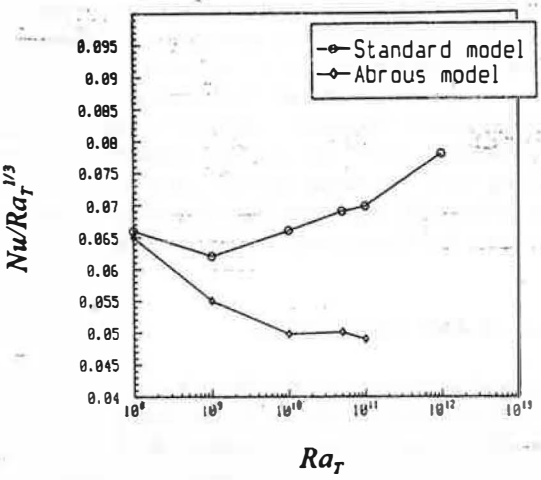

FIGURE 3 : EVOLUTION OF AVERAGE NUSSELT NUMBER AT HOT WALL AS A FUNCTION OF THE THERMAL RAYLEIGH NUMBER.

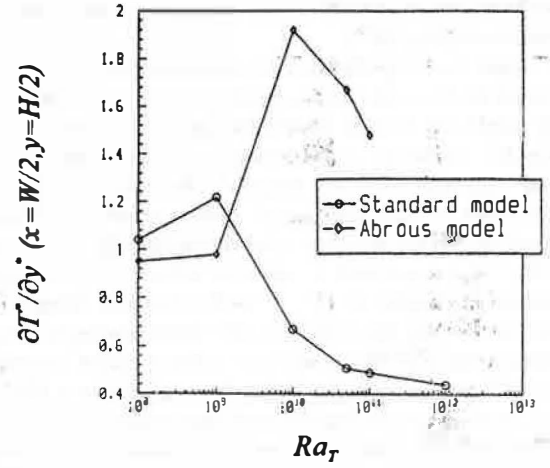

FIGURE 4 : EVOLUTION OF THE THERMAL STRATIFICATION $\partial T^*/\partial y^*$ AT CAVITY CENTER AS A FUNCTION OF THE THERMAL RAYLEIGH NUMBER.

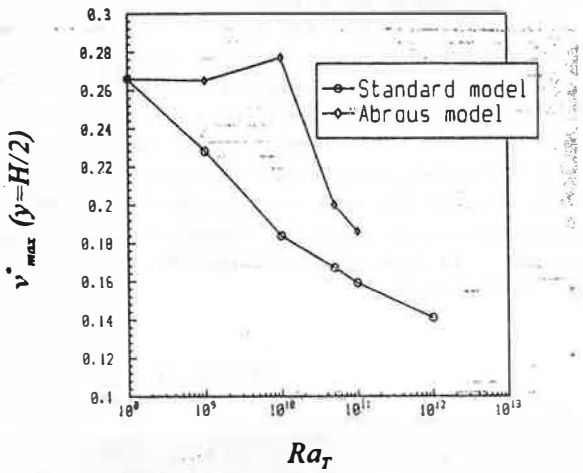

FIGURE 5 : EVOLUTION OF THE MAXIMUM VERTICAL VELOCITY AT HALF THE CAVITY HEIGHT AS A FUNCTION OF THE THERMAL RAYLEIGH NUMBER.

Some of the above mentioned remarks are stressed in Figures 6, 7, 8, 9, 10, 11 which represent the streamlines, isopleths of temperature and turbulent viscosity obtained with the Henkes and Hoogendoorn model and the Abrous model for a Rayleigh number range between 10^9 and 10^{11}. The fully turbulent regions are located at the top left and bottom right corners of the cavity where the shear stresses are high (Figures 8 and 11). For both models, these regions stretch along the vertical walls for increasing values of the thermal Rayleigh number. The main differences between these two patterns are much higher values of turbulent viscosity and more extended fully turbulent regions predicted by the Henkes and Hoogendoorn model. In fully turbulent regions, the turbulent viscosity diffuses the average velocity and temperature fields. At the top left and bottom right corners of the cavity, the streamlines and temperature distorsions are smoothed by the turbulent viscosity (see Figures 6, 7, 9, 10). The hydraulic jumps present for the Abrous model at the top left and bottom right corners of the cavity for a thermal Rayleigh number of 10^9 disappear for higher values of the thermal Rayleigh number. One can also remark the decrease in the thermal and dynamic boundary layer thicknesses for increasing thermal Rayleigh numbers. The evolution of the thermal stratification at cavity center observed in Figure 4 is highlighted in Figures 7 and 10: a global decrease predicted by the Henkes and Hoogendoorn model, a decrease in the laminar range (Figures 10.a and b) and an increase in the turbulent range (Figure 10.c) for the Abrous model. Another difference to be emphasized between these two models is about the streamlines for a thermal Rayleigh number of 10^9. The Abrous model predicts hydraulic jumps while the Henkes and Hoogendoorn model does not: the turbulent viscosity predicted by the Abrous model is too weak to smooth out these hydraulic jumps. The last feature to notice is the larger thermal and dynamic boundary layer thicknesses for the Henkes and Hoogendoorn model, due to the stronger diffusion process induced by higher levels of turbulent viscosity.

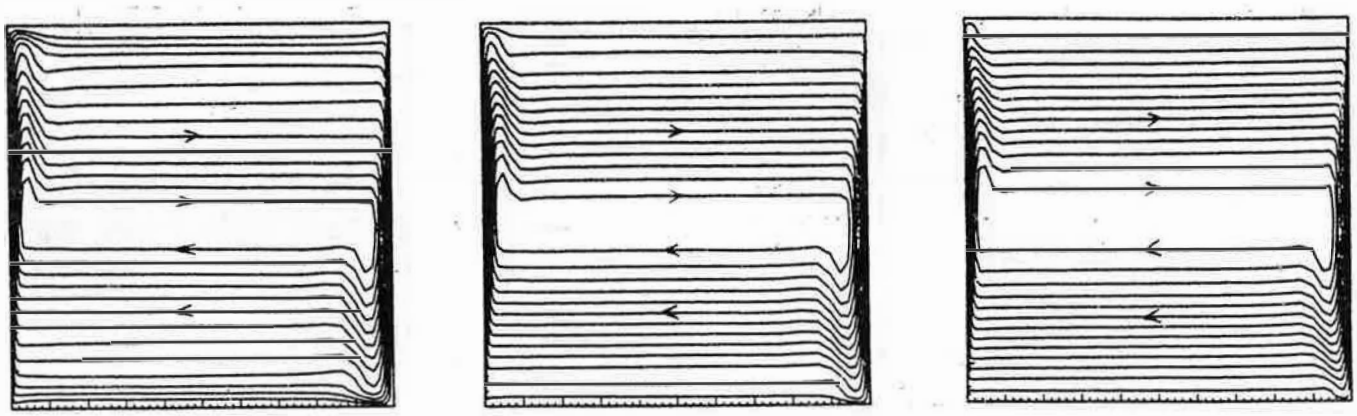

FIGURE 6 : STREAM FUNCTION ISOCONTOUR MAP (HENKES AND HOOGENDOORN MODEL).
Isovalues are (a) 0, (0.00035), 0.00461, (b) 0, (0.00034), 0.00438, (c) 0, (0.00022), 0.00284.

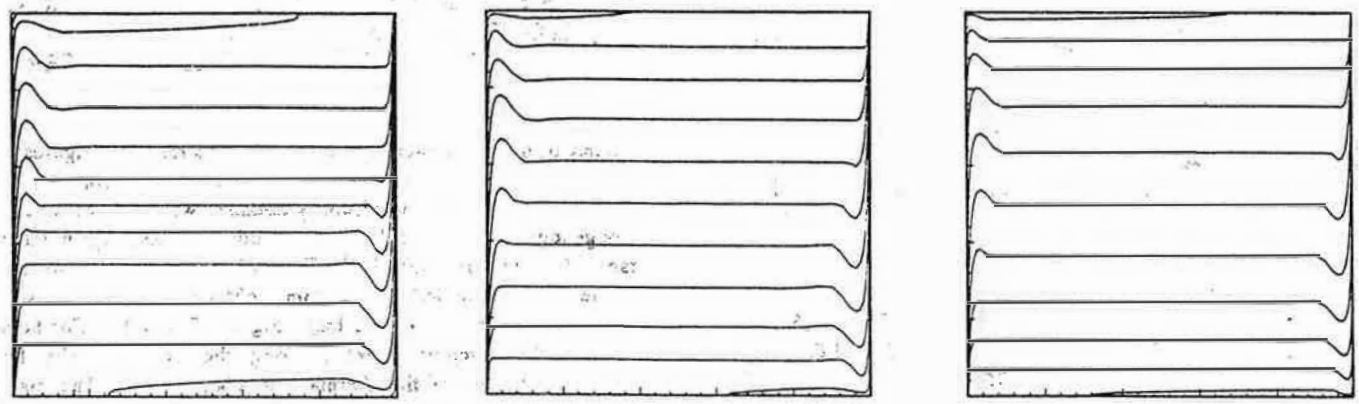

FIGURE 7 : ISOTHERMS (HENKES AND HOOGENDOORN MODEL).
Isovalues are (a), (b), (c) 0, (0.07143), 1.00000.

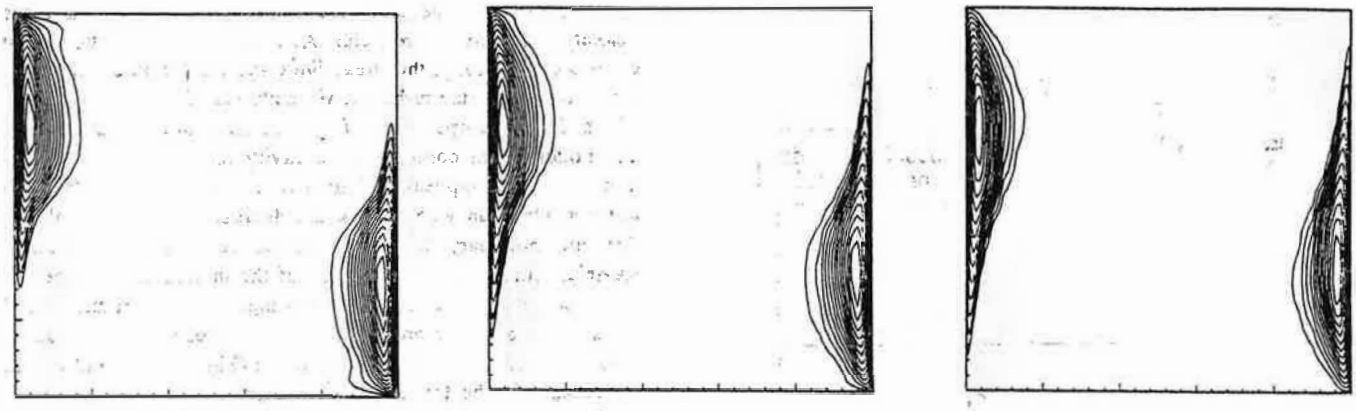

FIGURE 8 : TURBULENT VISCOSITY ISOCONTOUR MAP (HENKES AND HOOGENDOORN MODEL).
Isovalues are (a) 0, (0.656), 8.535, (b) 0, (2.414), 31.379, (c) 0, (16.62), 232.74.

(a) $Ra_T=10^8$ *(b)* $Ra_T=10^{10}$ *(c)* $Ra_T=10^{12}$

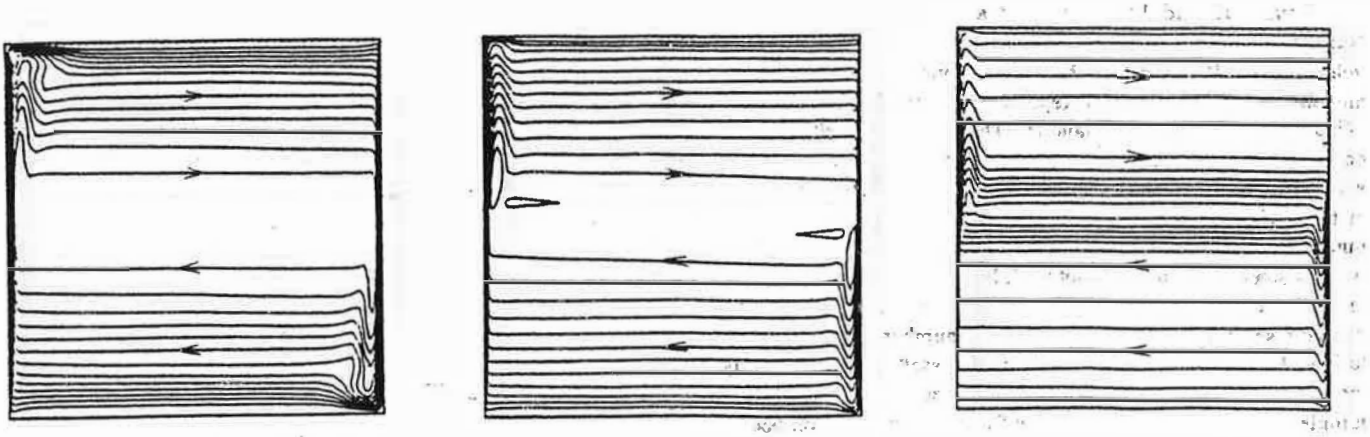

FIGURE 9 : STREAM FUNCTION ISOCONTOUR MAP (ABROUSMODEL).
Isovalues are (a) 0, (0.00026), 0.00342, (b) 0, (0.00017), 0.00224, (c) 0, (0.00015), 0.00199.

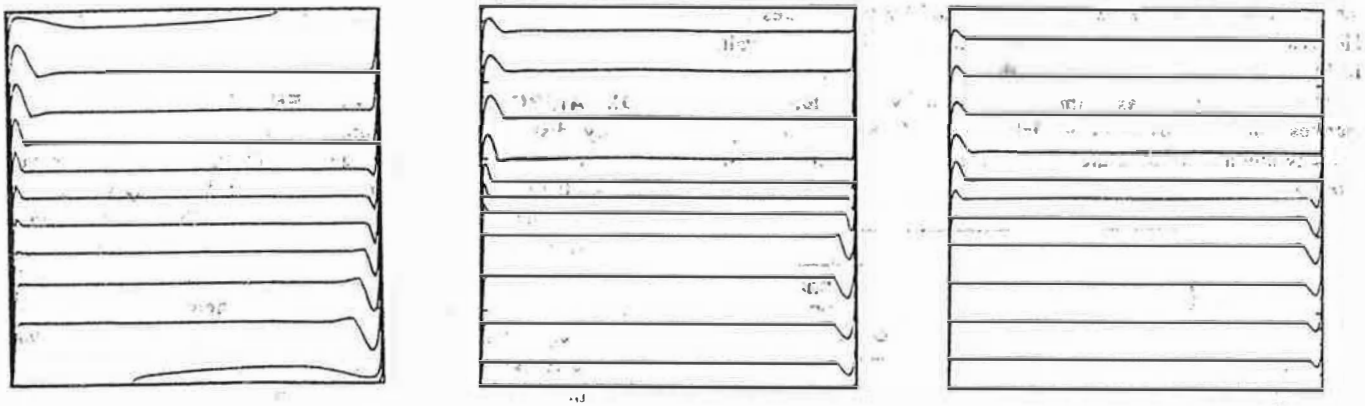

FIGURE 10 : ISOTHERMS (ABROUS MODEL).
Isovalues are (a), (b), (c) 0, (0.07143), 1.00000.

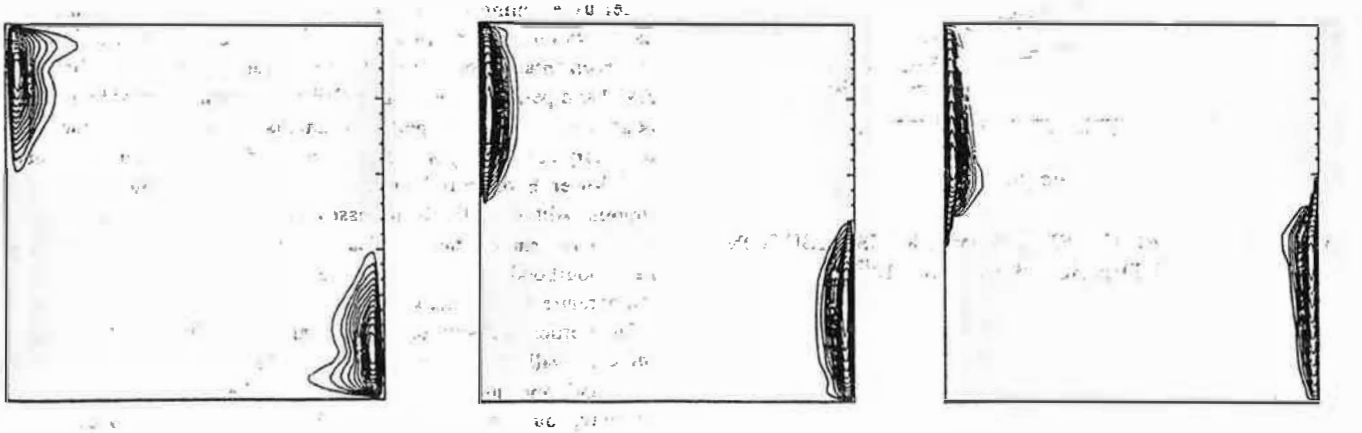

FIGURE 11 : TURBULENT VISCOSITY ISOCONTOUR MAP (ABROUS MODEL).
Isovalues are (a) 0, (0.451), 5.858, (b) 0, (1.11), 14.43, (c) 0, (2.973), 38.643.

(a) $Ra_T=10^9$ *(b)* $Ra_T=10^{10}$ *(c)* $Ra_T=10^{11}$

In Figures 12 and 13, we present a comparison of the local Nusselt number distribution at the hot wall and the vertical velocity at half the cavity height computed by the three k-ε models tested, for a thermal Rayleigh number of 10^{10} (Adiabatic Window Problem configuration). The local Nusselt number computed by the Chien model constantly decreases along the hot wall (Figure 12), the behavior of the flow is laminar everywhere in the cavity, the turbulent viscosity is zero everywhere. For the other two models, the local Nusselt number behaves differently in two distinct zones along the hot wall. In the laminar region located in the lower part of the hot wall, the high temperature gradients induce a sharp decrease in local Nusselt number. In the laminar-turbulent transition region, the local Nusselt number slightly increases and decreases in a less pronounced manner in the fully turbulent region, due to the strong diffusion process which occurs in this region. Moreover, as for identical Rayleigh numbers the fully turbulent region predicted by the Henkes and Hoogendoorn model is widest than the one predicted by the Abrous model, the laminar-turbulent transition region predicted by the Henkes and Hoogendoorn model is located closer to the lower horizontal wall. In Figure 13, one clearly remarks the thicker dynamic boundary layer and the lower maximum vertical velocity predicted by the Henkes and Hoogendoorn model which diffuses the average velocity much more than the two other low-Reynolds number k-ε models.

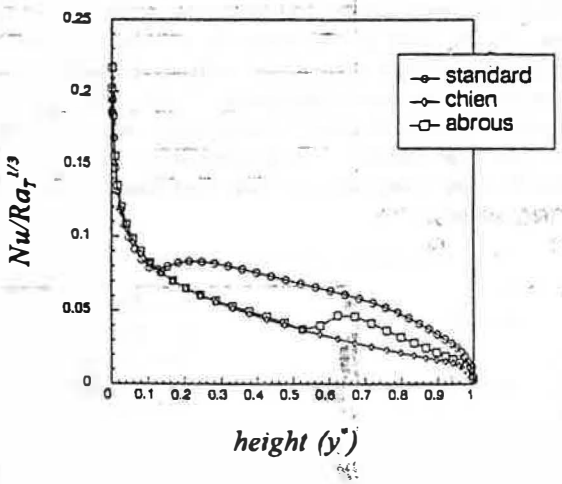

FIGURE 12 : LOCAL NUSSELT NUMBER DISTRIBUTION ALONG THE HOT WALL ($Ra_T=10^{10}$).

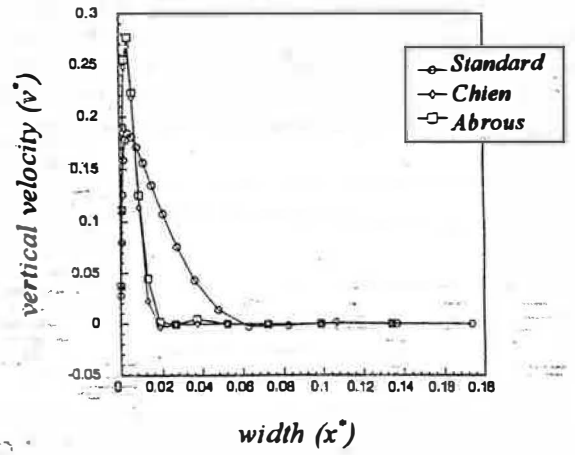

FIGURE 13 : VERTICAL VELOCITY AT HALF THE CAVITY HEIGHT ($Ra_T=10^{10}$).

COMPARISON WITH EXPERIMENTAL RESULTS

Many distributions were provided by the experiments (for additional information, see Mergui et al. (1992)). Among these we selected the temperature distribution at half the cavity width, the vertical velocity and temperature profiles at half the cavity height, the local Nusselt number distribution along the vertical walls. Three numerical simulations have been carried out. For a thermal Rayleigh number of 1.7×10^9, a cavity height and a width respectively equal to 0.94 m and 1.04 m (as in the experimental cell), the Henkes model and the Abrous model have been used. While the horizontal walls were considered adiabatic for the Henkes model, they were either adiabatic or perfectly conductive for the Abrous model.

Let us examine first the temperature distributions at half the cavity width (Figures 14 a and b). The determining influence of the horizontal thermal boundary conditions (perfectly adiabatic AWP and perfectly conductive CWP numerical thermal boundary conditions, vs almost perfectly adiabatic experimental thermal boundary conditions) on the temperature distributions in the upper and lower horizontal boundary layers is highlighted in these figures. Although the heat losses through the cavity walls are extremely small, the vertical temperature gradient in the neighbourhood of the horizontal walls greatly affects the temperature distributions in these regions.

The vertical velocity profiles at half the cavity height (close to the cold wall) are presented in Figure 15. While the Henkes and Hoogendoorn model underestimates the maximum vertical velocity, due to the strong turbulent diffusion process, the agreement with the experimental profile is rather good for the Abrous model (AWP and CWP). One must also remark the location of the maximum vertical velocity given by the experiment, which is closer to the cold wall than those computed. For x^* smaller than 0.01, the experimental and numerical temperature distributions at half the cavity height and close to the hot wall (see Figure 16) are almost identical. As noticed in the experimental profile, the temperature is diffused by the Henkes

model (AWP). The Abrous model (AWP and CWP) predicts a smaller recirculation region closer to the solid boundary than the Henkes model (AWP), which does not exist in the experiment. In the core of the cavity, the experimental temperature level is 0.52, which is a little higher than the computed temperature levels.

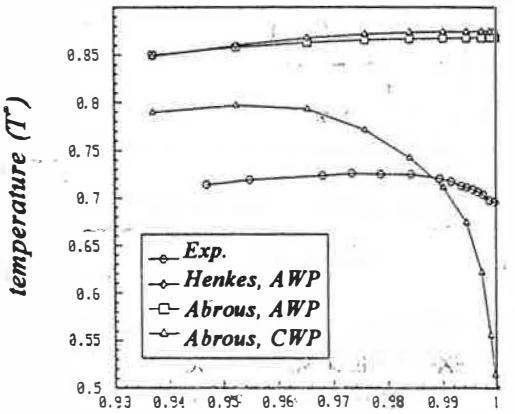

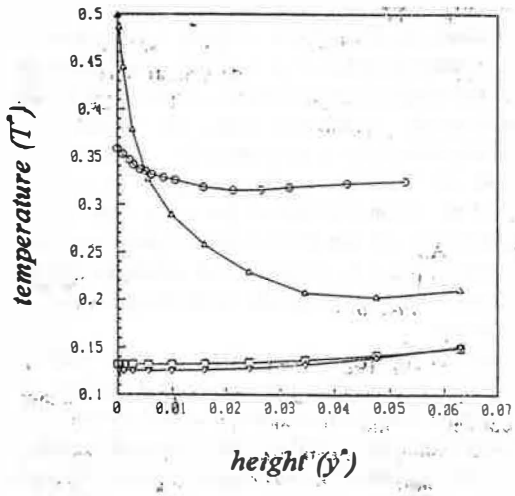

FIGURE 14 : EXPERIMENTAL AND COMPUTED TEMPERATURE DISTRIBUTIONS AT HALF THE CAVITY WIDTH (a) UPPER WALL, (b) LOWER WALL.

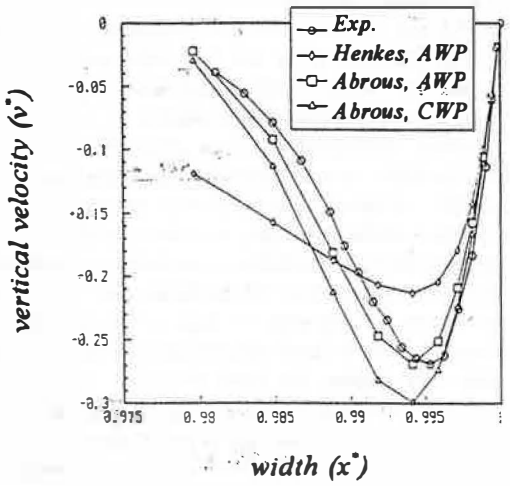

FIGURE 15 : EXPERIMENTAL AND COMPUTED VERTICAL VELOCITY PROFILES AT HALF THE CAVITY HEIGHT (CLOSE TO THE COLD WALL).

An investigation of the local Nusselt number distributions along the vertical walls stresses the strong influence of the thermal boundary conditions imposed at horizontal walls on the flow (Figure 17). In spite of the relatively uniform temperatures experimentally imposed at horizontal walls, the best concordance between computations and experiments is found for the "Perfectly Conductive Window Problem" configuration and the Abrous model. The heat transfer is overestimated for the "Adiabatic Window Problem" computations (Henkes and Hoogendoorn model and Abrous model).

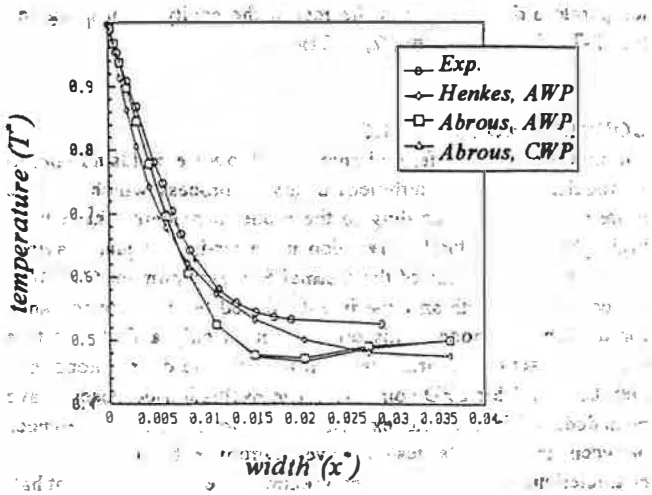

FIGURE 16 : EXPERIMENTAL AND COMPUTED TEMPERATURE DISTRIBUTIONS AT HALF THE CAVITY HEIGHT (CLOSE TO THE HOT WALL).

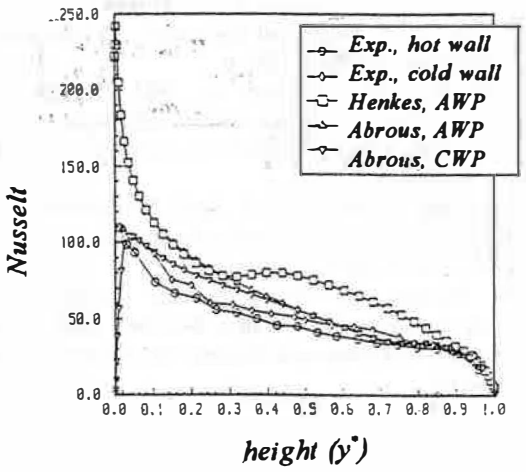

FIGURE 17 : EXPERIMENTAL AND COMPUTED LOCAL NUSSELT NUMBER DISTRIBUTIONS ALONG VERTICAL WALLS.

Models	*HENKES (AWP)*	*ABROUS (AWP)*	*ABROUS (CWP)*	*Experiment*
V^*max $(y=H/2)$	0.213 $x^*=0.0059$	0.269 $x^*=0.0059$	0.299 $x^*=0.0059$	0.27 $x^*=0.005$
Nu	74.17	63.86	55.59	hot wall 52.7 cold wall 56.6
Stratification $\partial T^*/\partial y^*$ *at center*	1.09	0.998	0.87	0.37
T^* $(W/2,3H/4)$	0.713	0.734	0.706	0.61
Nu $(0,H/2)$	76.83	54.05	53.82	hot wall 48.5 cold wall 54.9

TABLE 1 : EXPERIMENTAL AND COMPUTED CHARACTERISTIC RESULTS.

The previous observations are summed up in Table 1, which collects experimental and computed characteristic results. The maximum vertical velocity at half the cavity height computed with the Abrous model, the average Nusselt number integrated over the hot wall and the local Nusselt number at mid-height of the hot wall obtained for the "Perfectly Conductive Window Problem" configuration with the Abrous model show a good agreement with the experimental findings. Even though the experimental thermal stratification at cavity center is much smaller than the computed ones, and despite the rather different temperature distributions in the horizontal boundary layers, experimental and computed temperature distributions in the rest of the cavity seem to agree (cf $(T-T_C)/(T_H-T_C)$ at x=W/2, y=3H/4).

CONCLUDING REMARKS

In this paper, the different behaviors of low-Reynolds number k-ε models, due to the turbulent diffusion process which may be more or less high according to the model considered, have been highlighted, for natural convection in an air-filled square cavity.

For a moderate value of the thermal Rayleigh number (1.7×10^9), the comparison with an experiment showed the best concordance for the Abrous model. This comparison is only a first step to a more accurate one. Horizontal wall temperature distributions, that may be useful for CFD computer code evaluation purposes, have been deduced from further experimental investigations. Differences between the models tested have moreover been noticed for characteristic values such as the maximum vertical velocity at half the cavity height, the average heat transfer rate, the thermal stratification at cavity center, which seem to be due to non identical transitions to unsteady natural convection predicted by these models. Further experimental investigations at higher thermal Rayleigh numbers are therefore necessary to validate numerical models.

ACKNOWLEDGEMENTS

Computations were performed on the IBM3090 supercomputer of the Centre National Universitaire Sud de Calcul (CNUSC) of Montpellier, France, within the frame of the C3NI (Centre de Compétence en Calcul Numérique Intensif).

REFERENCES

Abrous, A., Emery, A.F., Kazemzadeh, F., 1984, "Turbulent frec convection in rooms in the presence of drafts, cold windows and solar radiation". *Proceedings of the Symposium on Heat Transfer in Enclosures, Winter Annual Meeting of ASME*, New Orleans, Louisianne, december 9-14, 1984. ASME Paper, Vol.39, p.39-48.

Allard, F., Draoui, A., Béghein, C., 1991, "Quelques phénomènes convectifs naturels en milieu industriel: du refroidissement des circuits électroniques au tunnel sous la Manche". *Rev. Gén. Therm. Fr.*, No. 356-357, august-september 1991, p.499-507.

Allard, F., Béghein, C., Haghighat, F., 1992, "Utilisation des codes de mécanique des fluides comme outils de recherche et de conception". *Qualité de l'Air, Ventilation et Economies d'Energie dans les Bâtiments, Proceedings des Cinquièmes Entretiens du Centre Jacques Cartier*, Montréal, Canada, october 7-9, 1992. 16p.

Anderson, D.A., Tannehill, J.C., Pletcher, R.H., 1983, "Computational fluid mechanics and heat transfer". Washington: Hemisphere, 1983. 599 p.

Béghein, C., 1992, "Contribution à l'étude numérique de la convection naturelle thermosolutale en cavité. Application à la diffusion de polluants dans les pièces d'habitation". Thèse de Doctorat: Institut National des Sciences Appliquées de Lyon, 1992. 250p.

Béghein, C., Allard, F., Draoui, A., 1992, "Numerical modelling of turbulent convection in a thermally driven square cavity". *Proceedings of the Joint Workshop of EUROTHERM and ERCOFTAC : Turbulent Natural Convection in Enclosures, A Computational and Experimental Benchmark Study*. Delft, The Netherlands, march 25-27, 1992. Paris, France: Editions Européennes de Thermique et Industrie. 12 p.

Betts, P.L., Dafa'Alla, A.A., 1986, "Turbulent bouyant air flow in a tall rectangular cavity". *Significant questions in buoyancy affected enclosure or cavity flows, Proceedings of the ASME Winter Annual Meeting*, Anaheim, Califomie, december 7-12, 1986. Vol.60, p.83-91.

Cheesewright, R., Ziai, S., 1986, "Distributions of temperature and local heat transfer rate in turbulent natural convection in a large rectangular cavity". *Proceedings of the 8th International Heat Transfer Conference*, San Francisco, 1986. Vol.4, p.1465-1470.

Chen, Q., Moser, A., Huber, A., 1990, "Prediction of buoyant, turbulent flow by a low Reynolds number k-ε model". *ASHRAE Transactions*, 1990, Vol.96, Part 1, 10p.

Chien, K.Y., 1982, "Predictions of channel and boundary layer flows with a low-Reynolds-number turbulence model". *AIAA Journal*, 1982, Vol.20, p.33-38.

Fraikin, M.P., Portier, J.J., Fraikin, C.J., 1980, "Application of a k-ε turbulence model to an enclosed buoyancy driven recirculating flow". *Joint ASME/AIChE National Heat Transfer Conference*, Orlando, July 27-30, 1980. ASME paper 80-HT-68. 12p.

Henkes, R.A.W.M., Hoogendoorn, C.J., 1992, "Contribution of the Heat Transfer Group at the J.M. Burgers Centre". *Proceedings of the Joint Workshop of EUROTHERM and ERCOFTAC : Turbulent Natural Convection in Enclosures, A Computational and Experimental Benchmark Study*. Delft, The Netherlands, march 25-27, 1992. Paris, France: Editions Européennes de Thermique et Industrie. 12 p.

Jones, W.P., Launder, B.E., 1972, "The prediction of laminarization with a two-equation model of turbulence". *International Journal of Heat and Mass Transfer*, 1972, Vol.15, p.301-313.

Lam, C.K.G., Bremhorst, K., 1981, "A modified form of the k-ε model for predicting wall turbulence". *Journal of Fluids Engineering*, 1981, Vol.103, p.456-460.

Lankhorst, A., 1991, "Laminar and turbulent natural convection in cavities. Numerical modelling and experimental validation". Ph.D. thesis: Delft University, The Netherlands, 1991. 246 p.

Launder, B.E., Sharma, B.I., 1974, "Application of the energy dissipation model of turbulence to the calculation of flow near a spinning disc". *Letters in Heat and Mass Transfer*, 1974, Vol.1, p.131-138.

Mergui, S., Penot, F., Tuhault, J.L., 1992, "Experimental natural convection in an air-filled square cavity at $Ra=1.7\times10^9$". *Proceedings of the Joint Workshop of EUROTHERM and ERCOFTAC : Turbulent Natural Convection in Enclosures, A Computational and Experimental Benchmark Study*. Delft, The Netherlands, march 25-27, 1992. Paris, France: Editions Européennes de Thermique et Industrie. 12 p.

Nobile, E., Souza, A.C.M., Barozzi, G.S., 1989, "Turbulence modelling in confined natural convection". *Journal of Heat and Technology*, 1989, Vol.7, No.3-4, p.24-35.

Patankar, S.V., 1980, "Numerical heat transfer and fluid flow". Londres: Mac Graw Hill, 1980. 197 p.

Patel, V.C., Rodi, W., Scheuerer, G., 1981, "Evaluation of turbulence models for near wall and low Reynolds number flows". *3rd Symposium on Turbulent Shear Flows*, Califomia, 1981. p.1-8.

Patel, V.C., Rodi, W., Scheuerer, G., 1985, "Turbulence models for near-wall and low Reynolds number flows: A review". *AIAA Journal*, 1985, Vol.23, No.9, p.1308-1319.

Tsuji, T., Nagano, Y., 1989, "Velocity and temperature measurements in a natural convection boundary layer along a vertical flat plate". *Experimental Thermal Fluid Sciences*, 1989, Vol.2, p.208-215.